Photoexcited Molecular Structure of Diplatinum (II) Complex by Single-Crystal X-ray Structure Analysis

Direct observation of geometrical changes following photo-excitation of molecules provides essential information on transient species such as metastable states of chemical reactions and excited states, which are sometimes difficult to describe by molecular orbital calculations. Although single-crystal X-ray structure analysis is a powerful and conventional tool for obtaining accurate molecular geometry and structural parameters, there are some difficulties to be overcome to determine the structure of photo-excited molecules using ordinary diffractometers. Because of the extremely small populations and small geometrical changes of excited-state molecules in crystals, photo-excited crystallography requires more accurate measurements of diffraction intensities. We have developed a new low-temperature vacuum (LTV) X-ray camera installed on beamline **BL02B1** (Fig. 1), in addition to a special data collection system, the multiple-exposure IP method for excited-state crystallography. We report here the instrumentation and its first application to the luminescent diplatinum(II) $[Pt_2(pop)_4]^{4-}$ complex.
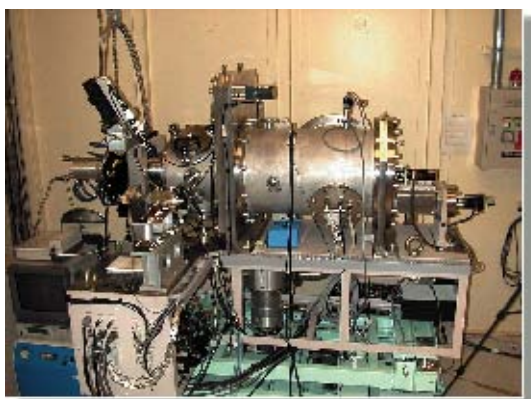
Fig. 1. Low-temperature vacuum X-ray camera.

The LTV camera is specially designed for accurate diffraction measurements with high S/N ratios at low temperature (< 80 K). To obtain diffraction images with extremely low background, an image plate (IP) is placed in a vacuum chamber preventing X-ray scattering from air and vacuum windows. A crystal specimen is mounted on a cold head of He refrigerator and can be cooled down to 20 K under a high vacuum. Crystal rotation, IP positioning, and the IP readout system are fully computer controlled for phi-oscillation and screenless Weissenberg modes. An additional feature of this camera is the multiple-exposure mode, in which both diffraction patterns under light-irradiated (light-on) and non-irradiated (light-off) conditions are recorded on the same IP frame. The first exposure by phi-oscillation mode under the light-off condition is followed by the second one under the light-on condition after a slight shift (1 to 2 mm) of the IP holder, and these processes are repeated several times to minimize systematic errors in the intensity measurements (Fig. 2). The doubly-recorded diffraction images can be read at the same time under the same conditions, giving accurate measurements of intensity change for each reflection. A laser light for photo-excitation can be introduced through fiber optics into the vacuum chamber and focused on the crystal (Fig. 3).

The $[Pt_2(pop)_4]^{4-}$ complex ion consists of two Pt(II) atoms bridged by four pyrophosphate ligands (Fig. 4). Two PtP_4 square planer moieties are stacked with an eclipsed configuration, and the Pt-Pt distance is 2.93 Å. Formally, there are no direct metal-metal bonds. Spectroscopic investigations of the complex show strong green luminescence,

light-off   **light-on
(with offset)**   **Multiple-exposed image**
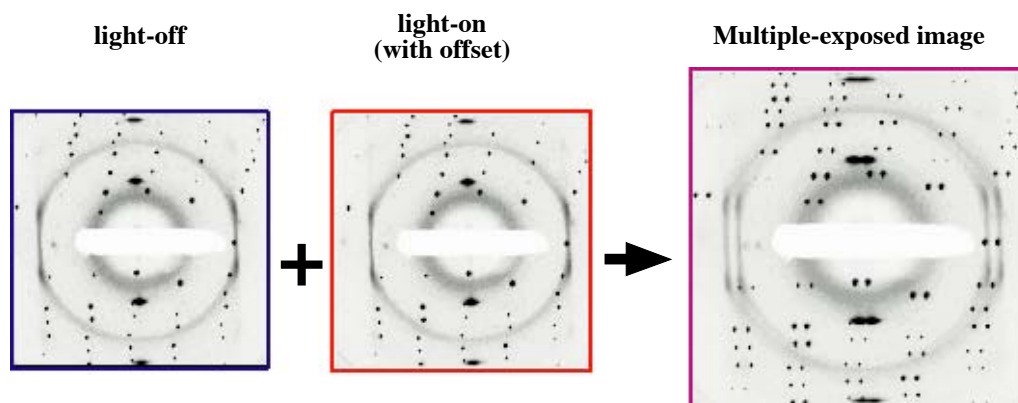

Fig. 2. Multiple-exposure IP method. The first X-ray exposure is followed by the second one after a 1 - 2 mm shift of the IP holder without readout or erasing processes. The doubly-recorded images are read at one time.

which has been attributed to $^3A_{2u} \to {}^1A_{1g}$ phosphorescence [1]. Emission spectra of the Ba^{2+} salts at 5 K exhibit fine structures with a spacing of 150 cm^{-1}, which are assigned to Pt-Pt stretching vibration in the $^3A_{2u}$ excited state [2]. The frequency of the vibrational structure in the excited states is higher than that in the ground state (116 cm^{-1}), suggesting an effective Pt-Pt bond formed in the excited states. The $^1A_{1g} \to {}^1A_{2u}$ absorption corresponds to the $5d\,\sigma^* \to 6p\,\sigma$ electronic transitions.

A single crystal of $(n\text{-Bu}_4\text{N})_2\text{H}_2[\text{Pt}_2(\text{pop})_4]$ situated on top of carbon fiber supports was mounted on the camera, and was kept at 54 K. A He-Cd blue CW laser (442 nm / 100 mW) was used for photo-excitation, continuously illuminating during the light-on period to maintain the crystal in a

pseudo-steady state. The multiple-exposure oscillation photo comprising alternating light-off and light-on periods for 24 seconds each was repeated ten times to record one IP frame. 52 frames of oscillation photo were subjected to intensity data processing. Standard crystal structure analyses were performed using each light-on and light-off intensity data sets independently. Lattice constants for the light-on data set were slightly larger than that for the light-off set. However, standard structural analysis showed that there were no differences in atomic parameters except an increase in temperature factors for the light-on data set. These results indicate that the heating effect by laser irradiation has caused a small temperature rise that led to expansion of the unit-cell volume in the light-on condition.
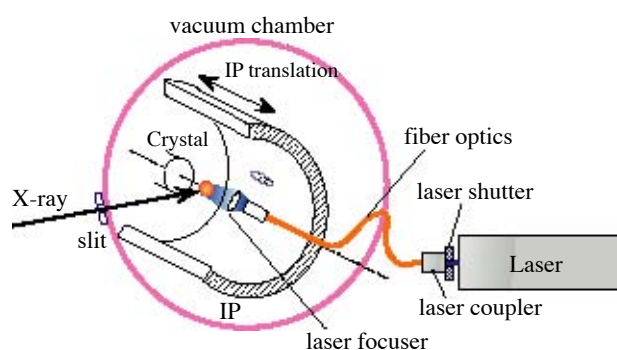

Fig. 3. Schematic layout of the LTV camera with laser irradiation optics.

To reveal small changes of crystal structure between the light-on and light-off data sets, difference Fourier syntheses were performed for $|F_{on}| - |F_{off}|$ using the phase factors calculated by the atomic parameters of the light-off data set. The observed electron density map (Fig. 4) shows positive and negative peaks with heights of 1 - 2 $e/Å^3$ near the Pt atoms, indicating that a small portion of the metal atoms moves toward the positive peaks in the light-on crystal. The Pt(1) atom shifts toward the Pt(2) position, while the Pt(2) atom shifts within the plane perpendicular to the Pt-Pt vector. These results clearly reflect shrinkage in the Pt-Pt distance. Changes in the geometrical parameters of the Pt atoms were analyzed quantitatively by least-squares calculations based on the response ratio (defined as $\eta = (I_{on} - I_{off})/I_{off}$) [3]. The positional and occupancy parameters of the Pt atoms in the excited states reveal that the Pt(1*)–Pt(2*) distance in the excited state is 2.70 (4) Å, which is 0.23 Å shorter than that of the ground state (Pt(1)–Pt(2) 2.9289 (2) Å) [4].
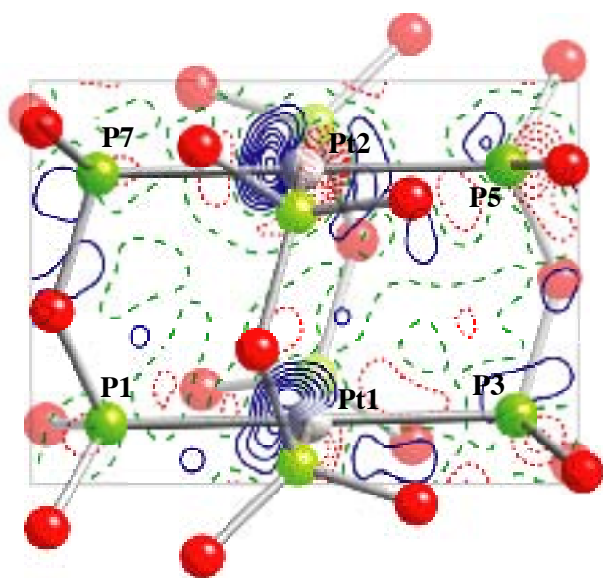

Fig. 4. Difference Fourier map (superimposed with a molecular diagram) of $|F_{on}| - |F_{off}|$ in a plane containing Pt(1)–Pt(2) vector and coordinated four P atoms of the ligands. Continuous lines and dashed lines indicate positive and negative density, drawn at every 0.2 $e/Å^3$, respectively.

Yoshiki Ozawa and Koshiro Toriumi

Himeji Institute of Technology

E-mail: toriumi@sci.himeji-tech.ac.jp

References

[1] D. M. Roundhill *et al.,* Acc. Chem. Res. **22** (1989) 55.
[2] A. P. Zipp, Coord. Chem. Rev. **84** (1988) 47.
[3] Y. Ozawa *et al.* , J. Appl. Cryst. **31** (1998) 128.
[4] Yoshiki Ozawa, Madoka Terashima, Minoru Mitsumi, Koshiro Toriumi, Nobuhiro Yaduda, Hidehiro Uekusa and Yuji Ohashi, Chem. Lett. **32** (2003) 62.